CHEMISTRY
A EUROPEAN JOURNAL

DOI: 10.1002/chem.201001281

Hypervalent Silicon Compounds by Coordination of Diphosphine–Silanes to Gold

Pauline Gualco,[a] Maxime Mercy,[b] Sonia Ladeira,[c] Yannick Coppel,[d] Laurent Maron,*[b] Abderrahmane Amgoune,*[a] and Didier Bourissou*[a]

Abstract: Coordination of ambiphilic diphosphine–silane ligands [*o*-(*i*Pr$_2$P)C$_6$H$_4$]$_2$Si(R)F (R = F, Ph, Me) to AuCl affords pentacoordinate neutral silicon compounds in which the metal atom acts as a Lewis base. X-ray diffraction analyses, NMR spectroscopy, and DFT calculations substantiate the presence of Au→Si interactions in these complexes, which result in trigonal-bipyramidal geometries around silicon. The presence of a single electron-withdrawing fluorine atom is sufficient to observe coordination of the silane as a σ-acceptor ligand, provided it is positioned *trans* to gold. The nature of the second substituent at silicon (R = F, Ph, Me) has very little influence on the magnitude of the Au→Si interaction, in marked contrast to N→Si adducts. According to variable-temperature and 2D EXSY NMR experiments, the apical/equatorial positions around silicon exchange in the slow regime of the NMR timescale. The two forms, with the fluorine atom in *trans* or *cis* position to gold, were characterized spectroscopically and the activation barrier for their interconversion was estimated. The bonding and relative stability of the two isomeric structures were assessed by DFT calculations.

Keywords: gold · hypervalent compounds · sigma-acceptor ligands · silicon · substituent effects

Introduction

The ability of Lewis acids to act as σ-acceptor ligands[1] has attracted growing interest over the past decade. The increasing number and variety of structurally authenticated transition-metal complexes of boranes, alanes, and gallanes have given more insight into unusual M→ER$_3$ interactions (E = B, Al, Ga).[2–3] Here, the combination of donor and acceptor moieties within the same ligand architecture, so-called ambiphilic ligands, proved particularly efficient. This approach provides straightforward access to complexes featuring coordinated Lewis acids, and the geometric constraints can be largely modulated by varying the number of donor buttresses and the nature of the spacers between the donor and acceptor sites.[4]

The scope of σ-acceptor ligands nowadays appears significantly broader than initially believed, and a great variety of complexes are in fact susceptible to such metal→Lewis acid interactions.[5] To assess to which extent the Lewis acidity of the σ-acceptor site can be decreased while retaining substantial interaction with the metal, we recently became interested in the coordination of saturated compounds of heavier Group 14 elements ER$_4$ (E = Si, Sn, …) to transition metals. The targeted metal→ER$_4$ interactions would arise from donation of an occupied d orbital at the metal to a vacant low-lying σ* orbital centered at silicon or tin. Pentacoordinate adducts of silanes and stannanes have been well documented with organic Lewis bases (N, O, S, …) in both intra- and intermolecular versions,[6] but related adducts with a transition metal acting as a Lewis base have scarcely been

[a] P. Gualco, Dr. A. Amgoune, Dr. D. Bourissou
University of Toulouse, UPS, LHFA
CNRS, LHFA UMR 5069, 118 route de Narbonne
31062 Toulouse (France)
Fax: (+33) 5-6155-8204
E-mail: amgoune@chimie.ups-tlse.fr
dbouriss@chimie.ups-tlse.fr

[b] Dr. M. Mercy, Dr. L. Maron
University of Toulouse, INSA, UPS, LPCNO
CNRS, LPCNO UMR 5215, 135 avenue de Rangueil
31077 Toulouse (France)
Fax: (+33) 5-6155-9697
E-mail: laurent.maron@irsamc.ups-tlse.fr

[c] S. Ladeira
Structure Fédérative Toulousaine en Chimie Moléculaire, FR 2599
118 route de Narbonne, 31062 Toulouse cedex 9 (France)

[d] Dr. Y. Coppel
Laboratoire de Chimie de Coordination, UPR8241 CNRS
205 route de Narbonne, 31077 Toulouse (France)

Supporting information for this article is available on the WWW under http://dx.doi.org/10.1002/chem.201001281.

studied. Grobe and co-workers prepared nickel and palladium cage complexes of type **A**,[7] but X-ray diffraction analyses revealed long M–Si distances and tetrahedral geometries around silicon, suggesting little, if any, M→Si interaction. In addition, the existence of donor–acceptor M→Si and M→Sn interactions has been invoked in silicon- and tin-bridged [1]ferrocenophanes **B**[8] as well as in silacyclotriyne nickel complexes **C**,[9] in which relatively short M–Si distances are imposed geometrically.

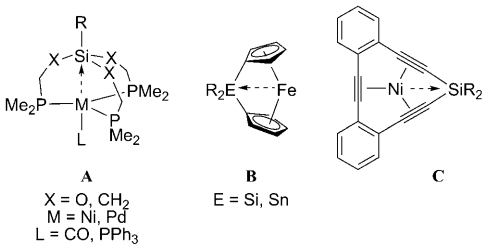

Recently, the ability of silanes and stannanes to behave as σ-acceptor ligands towards electron-rich transition metals was unambiguously substantiated by two independent studies. Wagler et al. isolated complexes of type **I** on reaction of tetramethimazolylsilanes and -stannanes with MCl_2 precursors (M = Pd or Pt).[10] Coordination is accompanied by the shift of a chlorine atom from the metal to the Group 14 element, and the transannular M→E (E = Si, Sn) interaction is supported by four methimazolyl buttresses, resulting in a lanternlike structure. Starting from diphosphine–silanes and stannanes, we prepared gold complexes of general formula **II**.[11] Here, the Au→E (E = Si, Sn) interaction is supported by only two phosphorus buttresses, and the heavier Group 14 element adopts a trigonal-bipyramidal arrangement. These preliminary results prompted us to explore the influence of the substitution pattern at silicon on the coordination of silanes as σ-acceptor ligands, and here we report a comprehensive study on a series of diphosphine–silane gold complexes [({*o*-(*i*Pr$_2$P)C$_6$H$_4$}$_2$Si(R)X)AuCl] (R = F, Ph, Me, X = F, Me). The presence and magnitude of the Au→Si interaction were assessed spectroscopically, structurally and theoretically.

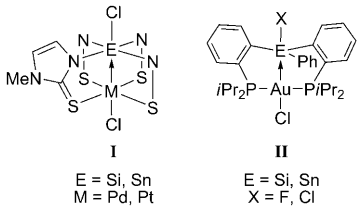

Results and Discussion

Diphosphine–silane ligands **1**–**3** were prepared by treating two equivalents of *o*-lithiated diisopropylphenylphosphine with the trichlorosilane $RSiCl_3$ (R = Ph, Cl, Me) in toluene at −78 °C, and then with HF·collidine (collidine = 2,4,6-trimethylpyridine) to achieve chlorine to fluorine exchange. The desired complexes **4**–**6** were obtained as analytically pure, white solids (ca. 88% yield) by treating **1**–**3** with [AuCl(SMe$_2$)] in dichloromethane at −78 °C (Scheme 1).

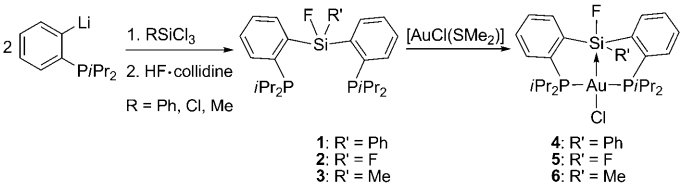

Scheme 1. Synthesis and coordination of diphosphine–silane ligands **1**–**3**.

Complex **4** was shown by X-ray diffraction analysis to feature an unusual Au→Si interaction, as discussed in a preliminary report.[11] The most diagnostic features are the short Au–Si distance of 3.090(2) Å, a geometry around the silicon center that only deviates slightly from trigonal-bipyramidal, and the noticeable elongation of the Si–F bond (from 1.599(7) Å in free ligand **1** to 1.635(3) Å in complex **4**). The pentacoordinate character of silicon in **4** was also apparent from NMR spectroscopic studies. In the solid state, the ^{29}Si NMR signal is shifted upfield on coordination, from $\delta = -5$ ppm in **1** to −23 ppm in complex **4**. Surprisingly, ^{19}F, ^{31}P, and ^{29}Si NMR analyses indicated the presence of two species in 60/40 ratio when the crystals of **4** were dissolved in $CDCl_3$. Based on the similarity of the ^{29}Si NMR chemical shifts, the major compound in solution ($\delta = -21.4$ ppm) was assigned to the structure observed in the solid state, with the fluorine atom *trans* to gold (**4**$_{trans}$). The ^{29}Si NMR chemical shift of the minor product ($\delta = -3.9$ ppm) differs significantly from that of **4**$_{trans}$, and is found in the same region as that of the free ligand. This suggests that the Au→Si interaction, if still present, is significantly weaker in this form. Another conspicuous feature of the minor species is the presence of a substantial P–F coupling constant (22.5 Hz). All these data are consistent with the minor species corresponding to the *cis* form **4**$_{cis}$ in which the fluorine atom is *cis* to gold (Scheme 2).

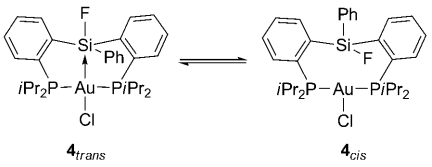

Scheme 2. Interconversion of the two isomeric forms **4**$_{trans}$ (major) and **4**$_{cis}$ (minor) in solution.

Variable-temperature ^{19}F and ^{31}P NMR studies were carried out to gain more insight into the interconversion of $\mathbf{4}_{trans}$ and $\mathbf{4}_{cis}$ in solution. The ratio between the two isomeric forms does not vary significantly from −20 to 60 °C, but dynamic exchange between $\mathbf{4}_{trans}$ and $\mathbf{4}_{cis}$ was apparent from broadening of the signals upon heating. However, decomposition occurred before coalescence, and as a result the activation barrier could not be readily estimated by using a modified Eyring equation.[12] We thus turned to 2D EXSY NMR experiments[13,14] to further substantiate the isomerization process around silicon, and to estimate the associated activation barrier. The cross-peaks observed between the resonance signals in the 2D $^{31}P\{^1H\}$ EXSY NMR spectrum (Figure 1) unambiguously indicate the presence of

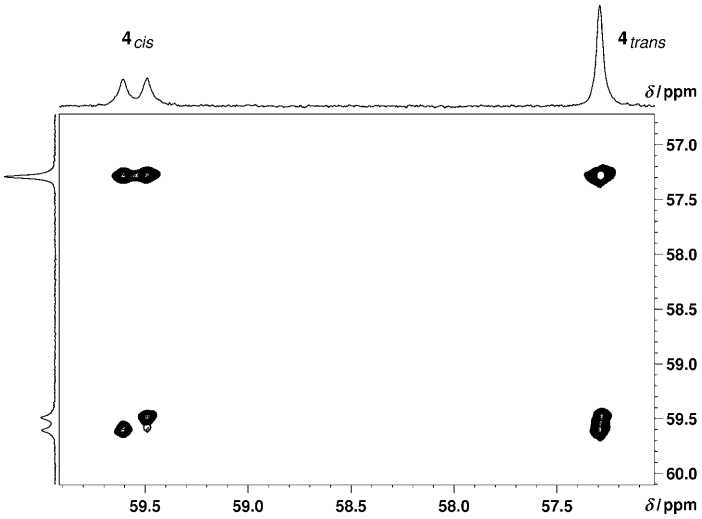

Figure 1. Contour plot of the 2D $^{31}P\{^1H\}$ EXSY NMR spectrum recorded for complex **4** at 277 K in $CDCl_3$ with a mixing time $t_m = 300$ ms.

dynamic exchange between the two species. The rate constant associated with the exchange process was calculated from the intensities of the cross-peaks according to the method of Perrin, Dwyer, and Gipe.[13,15] Accordingly, the activation barrier for the interconversion between $\mathbf{4}_{trans}$ and $\mathbf{4}_{cis}$ was estimated to be 14.9 kcal mol^{-1} at 277 K.

To gain some insight into the structure of $\mathbf{4}_{cis}$, DFT calculations were carried out at the B3PW91/SDD(Au,P,Cl), 6-31G**(Si,F,C,H) level of theory. In agreement with the experimental observations, two minima associated with the two arrangements around silicon were located at about the same energy on the potential surface ($\Delta G = 2.4$ kcal mol^{-1} in favor of $\mathbf{4}_{trans}$* at 25 °C; Figure 2).

The optimized structure of $\mathbf{4}_{trans}$* nicely reproduces that determined crystallographically (Table 1). The geometric data computed for the *cis* isomer $\mathbf{4}_{cis}$* differ significantly from those of $\mathbf{4}_{trans}$*: the Au–Si distance is much longer (3.45 Å in $\mathbf{4}_{cis}$* vs. 3.13 Å $\mathbf{4}_{trans}$*) and the geometry around the silicon center tends to tetrahedral rather than trigonal-bipyramidal ($\Sigma Si\alpha_{basal} = 341.3°$ and Au-Si-C_{Ph} 144.1° in $\mathbf{4}_{cis}$* vs. $\Sigma Si\alpha_{basal} = 356.9°$ and Au-Si-F 171.9° in $\mathbf{4}_{trans}$*). This is

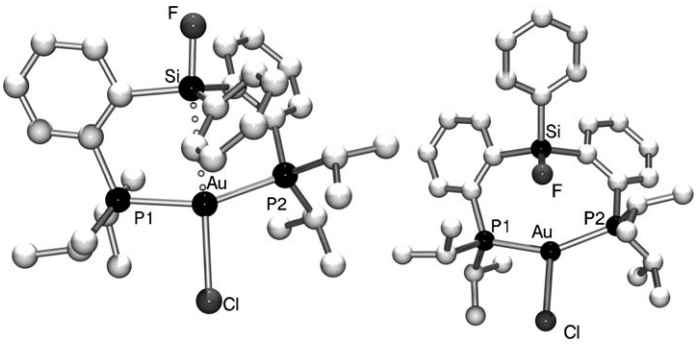

Figure 2. Optimized geometries of the two isomeric forms $\mathbf{4}_{trans}$ (left) and $\mathbf{4}_{cis}$ (right).

Table 1. Geometric data (bond lengths [Å] and angles [°]) determined crystallographically for complex $\mathbf{4}_{trans}$ and optimized computationally for actual complexes $\mathbf{4}_{cis}$* and $\mathbf{4}_{trans}$*.

	$\mathbf{4}_{trans}$ XRD	$\mathbf{4}_{trans}$* DFT	$\mathbf{4}_{cis}$* DFT
Au–Si	3.089(13)	3.131	3.452
Si–F	1.635(3)	1.663	1.634
Si–C_{Ph}	1.880(5)	1.890	1.892
Au-Si-X_{ap}	166.11(12)	171.86	144.08
$\Sigma Si\alpha_{basal}$	353.4(6)	356.86	341.33

consistent with the ^{29}Si NMR data and further supports weakening or even annihilation of the Au→Si interaction from $\mathbf{4}_{trans}$ to $\mathbf{4}_{cis}$.

The presence and magnitude of Au→Si interactions in the two isomeric forms of complex **4** were assessed by natural bond orbital (NBO) and atom in molecules (AIM) analyses. At the second-order perturbation level, a donor–acceptor interaction from gold to silicon was found in $\mathbf{4}_{trans}$* with a delocalization energy ΔE_{NBO} of 7.6 kcal mol^{-1} (Figure 3). In addition, the AIM electron density map of

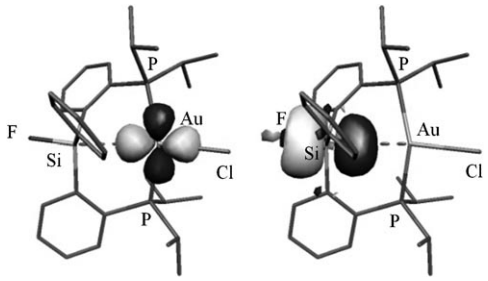

Figure 3. Molekel plots for the donor NBO (left) and acceptor NBO (right) associated with the Au→Si interaction in $\mathbf{4}_{trans}$.

$\mathbf{4}_{trans}$* shows the presence of a bond path between Au and Si with an electron density $\rho(r)$ of 2.13×10^{-2} e bohr^{-3} at the bond critical point (BCP). None of these features are observed for the isomer $\mathbf{4}_{cis}$*, that is, significant Au→Si interaction is absent in this form.

Comparison of the bonding situation in $\mathbf{4}_{trans}$ and $\mathbf{4}_{cis}$ substantiates the key role of the fluorine atom in the formation

of the Au→Si interaction, and draws some parallel with that known for neutral pentacoordinate adducts of silanes with organic bases. The σ^*_{SiF} orbital is substantially lower in energy than the σ^*_{SiPh} orbital. Consequently, coordination of the silane moiety as a σ-acceptor ligand is more favorable when the fluorine atom, rather than the phenyl group, is *trans* to gold (**4**$_{trans}$ rather than **4**$_{cis}$). These results also point out that the presence of the Au→Si interaction in **4**$_{trans}$, although supported by the two phosphorus buttresses, is not geometrically imposed by the structure of the ligand, since the silicon center moves away when the relative positions of the phenyl group and fluorine atom at silicon are exchanged.

To further investigate the influence of the substituents at silicon on the magnitude of metal→silane interactions, we then replaced the phenyl group by another electron-withdrawing fluorine atom. The solid-state structure of the ensuing complex **5** was elucidated by X-ray diffraction analysis (Figure 4). The silicon atom comes close to the metal center. The Au–Si distance (3.108(1) Å) is in between the sum of the covalent radii (2.47 Å)[16] and the sum of van der Waals radii (4.20 Å),[17] and actually very similar to that of **4**. The presence of a gold→silane interaction in **5** is further supported by the slightly distorted trigonal-bipyramidal geometry around silicon ($\Sigma Si\alpha_{basal} = 352.6°$). As a result, the two fluorine atoms become inequivalent. One fluorine atom, referred to as F_{ap}, occupies an apical position and is located approximately *trans* to gold (F_{ap}-Si-Au 164.38(8)°), while the other fluorine atom, referred to as F_{eq}, sits in the equatorial plane, *cis* to gold (F_{eq}-Si-Au 66.62(7)°). The apical Si–F bond (Si–F_{ap} 1.612(2) Å) is slightly elongated compared to the equatorial one (Si–F_{eq} 1.588(2) Å), in line with what is typically observed in difluorosilane adducts with organic bases.[18]

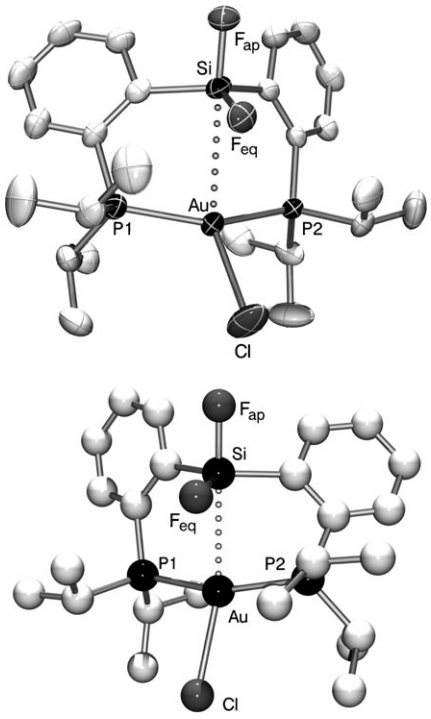

Figure 4. Top: Molecular view of **5** in the solid state (thermal ellipsoids set at 30% probability). Selected bond lengths [Å] and angles [°]: Au–Cl 2.600(1), Si–F_{eq} 1.588(2), Si–F_{ap} 1.612(2), Au–Si 3.108(1); P1-Au-P2 153.28(3), Cl-Au-Si 140.85(3), Au-Si-F_{ap} 164.38(8). Bottom: Optimized structure of **5***. In both cases, hydrogen atoms are omitted for clarity.

According to multinuclear NMR analyses, the Au→Si interaction is also present in solution. The ^{29}Si NMR chemical shift for **5** ($\delta = -37.3$ ppm) falls in the same range as those reported for pentacoordinate difluoro(diaryl)silicon derivatives featuring an intramolecular N→Si bond.[18a] The modification of the geometry around silicon upon coordination is also apparent from the ^{19}F NMR data. A single signal was observed at $\delta = -131.1$ ppm for free ligand **2**, but the two fluorine atoms are magnetically inequivalent in complex **5** ($\delta = -108.1$ and -125.4 ppm, $^2J(F,F) = 26$ Hz). The ^{19}F NMR chemical shifts observed for **4**$_{cis}$ ($\delta = -114.9$ ppm) and **4**$_{trans}$ ($\delta = -135.8$ ppm) support the following assignment for **5**: -108.1 ppm (F_{eq}) and -125.4 ppm (F_{ap}). Accordingly, only the fluorine atom in *cis* position to gold would exhibit a *J*-(P,F) coupling constant (14.7 Hz), in line with that observed for **4**$_{cis}$/**4**$_{trans}$. The elongation of the Si–F_{ap} bond as a result of d(Au)→σ*(SiF_{ap}) donation is probably responsible for the absence of P–F coupling for the fluorine atom *trans* to gold. The assignment of the ^{19}F NMR resonance signals of **5** was further confirmed by solid-state 2D HETCOR ^{31}P-^{19}F NMR spectroscopy. Here, the intensities of the cross-peaks due to ^{31}P–^{19}F dipolar coupling are directly related to the spatial proximity between the nuclei. For complex **5**, cross-peaks were observed for both ^{19}F NMR signals, with significantly higher intensity for that at -108.1 ppm.[19] This nicely agrees with the shorter distances observed in the solid state for P–F_{eq} (3.556 and 3.649 Å) versus P–F_{ap} (4.882 and 4.979 Å). In addition, variable-temperature ^{19}F NMR experiments revealed dynamic exchange of F_{ap} and F_{eq} in solution. The exchange proceeds in the slow regime of the NMR timescale up to temperatures at which decomposition occurs. The corresponding activation barrier, as estimated by 2D ^{19}F EXSY NMR spectroscopy ($\Delta G^{\ddagger} = 14.0$ kcal mol^{-1} at 283 K), is slightly lower than that determined for interconversion between **4**$_{cis}$ and **4**$_{trans}$.

Density functional theory (DFT) calculations were carried out on complex **5*** to shed more light into the Au→Si interaction. The optimized structure of **5*** nicely matches that determined experimentally for **5** (Figure 4), and NBO and AIM analyses further confirmed the presence of the Au→Si donor–acceptor interaction. The corresponding delocalization energy ($\Delta E_{NBO} = 8.1$ kcal mol^{-1}) and electron density $\rho(r)$ at the BCP (2.34×10^{-2} e bohr^{-3}) were found to be only slightly higher than those of **4**$_{trans}$, in agreement with the geometric data.

The structure of complex **5** confirms the propensity of diphosphine–silane ligands to engage in Au→Si interaction, and suggests that the silicon substituent in the equatorial position has minimal influence on the magnitude of the interaction. This behavior is in marked contrast with that of nitrogen adducts of fluorosilanes. Indeed, the strength of in-

tramolecular N→Si interactions typically increases with the number of fluorine atoms at silicon ($SiFPh_2 < SiF_2Ph < SiF_3$), as apparent from a significant shortening of the corresponding N–Si bond lengths.[18a]

To further assess the influence of the silicon substituents on the magnitude of the Au→Si interaction, complex **6** featuring a fluorine atom and a methyl group at silicon was then investigated. As previously observed, the coordination of the silane as a σ-acceptor ligand was unambiguously established by X-ray diffraction analysis (Figure 5). The Au–Si distance is short (3.089(3) Å) and the environment around silicon tends to trigonal-bipyramidal (Σ(C-Si-C) = 354.20(15)°). The fluorine atom occupies an apical position *trans* to gold (F-Si-Au 168.5(3)°), while the methyl group sits in the equatorial plane. Similarly to **4**, complex **6** adopts the $\mathbf{6}_{trans}$ form in the solid state. However, $\mathbf{6}_{trans}$ is the only species observed in solution in this case. The ^{29}Si NMR signal is shifted upfield by 16.5 ppm on coordination (from $\delta = 6.0$ ppm in the free ligand **3** to $\delta = -10.5$ ppm in $\mathbf{6}_{trans}$), and the ^{19}F NMR resonance appears as a singlet (no J(P,F) coupling constant) at $\delta = -141.5$ ppm.

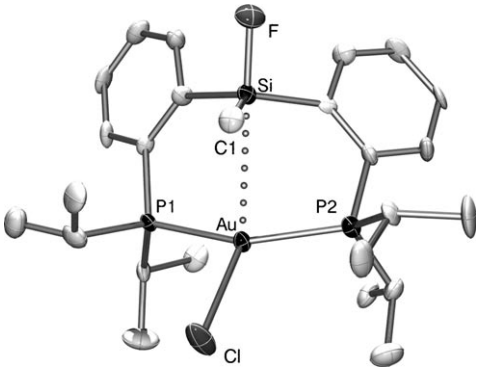

Figure 5. Molecular view of **6** in the solid state (thermal ellipsoids set at 50% probability and hydrogen atoms omitted for clarity). Selected bond lengths [Å] and angles [°]: Au–Cl 2.627(3), Si–F 1.639(7), Si–C1 1.873(11), Au–Si 3.089(3); P1-Au-P2 151.55(9), Cl-Au-Si 136.19(10), Au-Si-F 168.5(3).

DFT calculations were carried out on this complex as well to gain insight into the other conceivable form $\mathbf{6}_{cis}$* (featuring the fluorine atom in *cis* position to gold) and to compare the bonding situations in the two isomers. The optimized geometry of $\mathbf{6}_{trans}$* fits closely with that determined experimentally (Table 2). The $\mathbf{6}_{cis}$* isomer, not observed experimentally, was also found as a minimum on the potential-energy surface, about 4.1 kcal mol^{-1} higher in energy than $\mathbf{6}_{trans}$* (Figure 6). Similar to $\mathbf{4}_{cis}$*, the geometric features computed for $\mathbf{6}_{cis}$* substantiate the remoteness of the silicon atom from the gold center (the Au–Si distance is 3.425 Å and the environment around silicon tends to tetrahedral with $\Sigma Si_\alpha = 342.5°$). Furthermore, while the presence of an Au→Si interaction with similar magnitude to those of complexes $\mathbf{4}_{trans}$ and **5** was confirmed for $\mathbf{6}_{trans}$ by NBO ($\Delta E_{NBO} = 6.0$ kcal mol^{-1}) and AIM analyses ($\rho(r) = 1.89 \times 10^{-2}$ e bohr^{-3} at the bond critical point), such donor–acceptor interaction was not observed for $\mathbf{6}_{cis}$*.

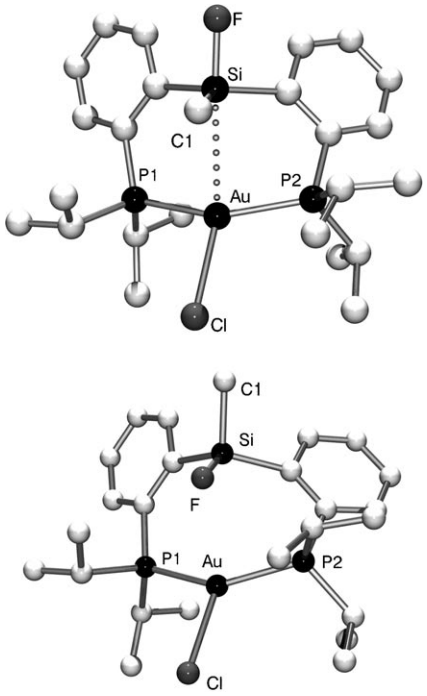

Figure 6. Optimized geometries of the two isomeric forms $\mathbf{6}_{trans}$ (top) and $\mathbf{6}_{cis}$ (bottom).

Table 2. Geometric data (bond lengths [Å] and angles [°]) determined crystallographically and optimized computationally for complex **6**.

	$\mathbf{6}_{trans}$ XRD	$\mathbf{6}_{trans}$* DFT	$\mathbf{6}_{cis}$* DFT
Au–Si	3.089(3)	3.061	3.425
Si–F	1.639(7)	1.703	1.665
Si–C_{Me}	1.873(11)	1.893	1.893
Au-Si-X_{ap}	168.5(3)	170.54	156.65
$\Sigma Si\alpha_{basal}$	354.20(15)	357.57	342.47

These results further confirm that the nature of the equatorial substituent at silicon has little, if any, influence on the magnitude of the Au→Si interaction in diphosphine–silane gold complexes such as **4**, **5**, and **6**. A single electron-withdrawing fluorine atom at silicon is enough to observe coordination of the silane as a σ-acceptor ligand, but its position plays a key role. Significant Au→Si interaction is only observed when the fluorine atom is positioned *trans* to the donor gold center and thus optimizes the overlap between the low-lying accepting orbital centered at silicon (σ^*_{SiF}) and the occupied donating d orbital at gold.

Finally, to confirm the necessity of an electron-withdrawing substituent to observe the coordination of the silane moiety as a σ-acceptor ligand, we sought to prepare and characterize a complex without fluorine at silicon. Diphosphine–silane ligand **7**, featuring two methyl substituents, was

prepared and coordinated to gold under similar conditions to the related fluorinated systems (Scheme 3).

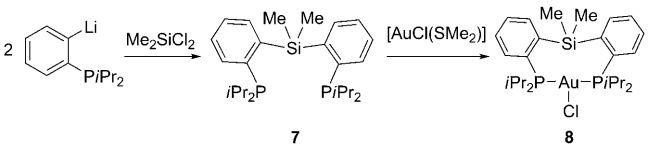

7 8

Scheme 3. Synthesis and coordination of diphosphine–silane ligand **7**.

Colorless crystals of complex **8** were obtained at −30 °C from dichloromethane/pentane, and an X-ray diffraction analysis was carried out (Figure 7). In contrast to complexes **4–6**, the solid-state structure of **8** exhibits a long Au–Si distance (3.345(1) Å), and the geometry around silicon remains essentially tetrahedral. The ^{29}Si NMR resonance signal is only slightly shifted upon coordination (from $\delta = -7.0$ ppm in free ligand **7** to $\delta = -12.4$ ppm in complex **8**), and falls in the same range as that observed in $\mathbf{4}_{cis}$. Moreover, the two methyl substituents at silicon remain magnetically equivalent in complex **8** (both in ^{1}H and ^{13}C NMR). All of these experimental data indicate that the silane moiety of **7** does not participate in coordination. The absence of Au→Si interaction in complex **8** was further substantiated by theoretical calculations. The key geometric features determined crystallographically were nicely reproduced computationally, and no sign of significant Au→Si interaction was found by NBO and AIM analyses.

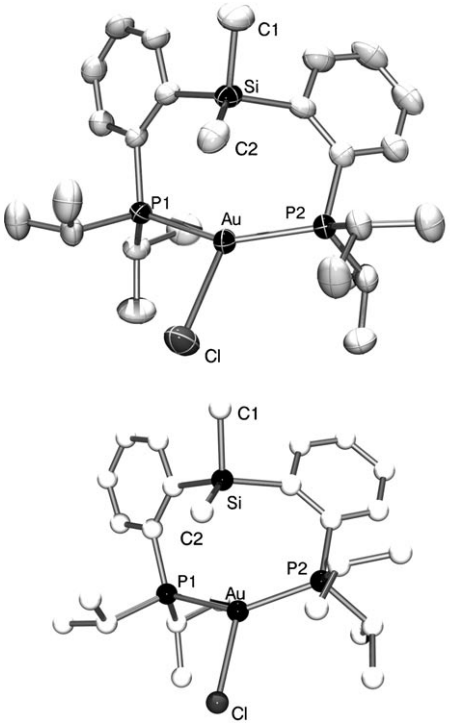

Figure 7. Top: molecular view of **8** in the solid state (thermal ellipsoids set at 50% probability). Selected bond lengths [Å] and angles [°]: Au–Cl 2.691(9), Si–C1 1.895(4), Si–C2 1.877(4), Au–Si 3.345(1); P1-Au-P2 148.33(3)°; Cl-Au-Si 136.15 (3)°; Au-Si-C1 164.52(14)°. Bottom: optimized structure of **8***. In both cases, hydrogen atoms are omitted for clarity.

Conclusion

Diphosphine–silane gold complexes **4–6** have been shown experimentally and theoretically to feature donor–acceptor Au→Si interactions. This study provides a comprehensive picture of the factors influencing the formation of pentacoordinate silicon derivatives in which a metal center acts as a Lewis base. In this series, the presence of a single electron-withdrawing fluorine atom is enough to observe coordination of the silane as a σ-acceptor ligand. The nature of the second substituent at silicon (R = F, Ph, Me) has very little influence on the magnitude of the Au→Si interaction, in marked contrast with that observed for related N→Si adducts.

The apical/equatorial positions around silicon were found to exchange in the slow regime of the NMR timescale, and the two isomeric forms of complex **4**, with the fluorine atom in *trans* or *cis* position to gold, were characterized spectroscopically.

These results extend the concept of σ-acceptor ligands beyond highly electron deficient moieties (such as Group 13 Lewis acids), and further increase the variety of bonding situations achievable with heavier Group 14 elements. Spectacular developments have been reported over the last decade for complexes featuring side-on Si–H[20] and Si–Si[21] σ bonds, strongly donating SiR_3 groups,[22] and M–Si double- and triple-bond character.[23] Coordination of silanes as σ-acceptor ligands offers a further possibility. The variety of complexes prepared in the past few years from the same diphosphine–silane ligand architecture $[o\text{-}(R_2P)C_6H_4]_2SiR'R''$ nicely illustrates this versatility (Scheme 4).[24]

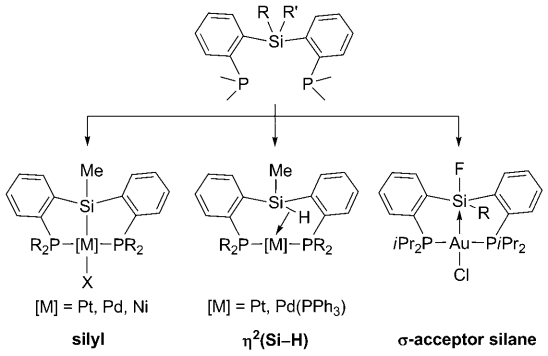

Scheme 4. Schematic representation of the various types of complexes prepared from diphosphine–silane ligands featuring *o*-phenylene backbones.

Experimental Section

All reactions and manipulations were carried out under an atmosphere of dry argon by using standard Schlenk techniques. Dry, oxygen-free solvents were employed. Solid-state ^{1}H, ^{13}C, ^{31}P, ^{19}F, ^{29}Si and 2D HETCOR ^{31}P,^{19}F NMR spectra were recorded on a Bruker Avance 400WB spectrometer. Solution ^{1}H, ^{13}C, ^{31}P, ^{19}F, ^{29}Si, ^{31}P, and ^{19}F 2D EXSY NMR spectra were recorded on Bruker Avance 300, 400, or 500 spectrometers. Chemical shifts are expressed in parts per million, relative to residual ^{1}H and ^{13}C solvent signals, 80% H_3PO_4, $CFCl_3$, or $SiMe_4$. The *N* values corresponding to $^{1}/_{2}[J(AX)+J(A'X)]$ are provided when second-order AA'X systems are observed in the ^{13}C NMR spectra.[25] Mass spectra were recorded on a Waters LCT apparatus. *o*-Lithiated diisopropylphenylphosphine was prepared by a previously described procedure.[4g] $SiCl_4$ and Me_2SiCl_2 were purchased from Aldrich and distilled before use. $MeSiCl_3$ (anhydrous beads, 97%) and $PhSiCl_3$ (anhydrous beads, 97%) were purchased from Aldrich and used as received. 2,4,6-Trimethylpyridine·2HF (HF·collidine) was purchased from Alfa Aesar and used as received.

Synthesis of diphosphine–silane 1: A solution of $SiPhCl_3$ (186 μL, 1.16 mmol) in toluene (5 mL) was added dropwise to a solution of *o*-lithiated diisopropylphenylphosphine (616 mg, 2.44 mmol) in toluene (5 mL) at −78 °C. The solution was allowed to warm slowly to room temperature over 4 h, after which the volatile substances were removed under vacuum, and the product was extracted from the salts with dichloromethane (10 mL) and directly used in the second-step reaction. A solution of HF·collidine (90 mg, 1.16 mmol) in dichloromethane (5 mL) was added to the product in dichloromethane (10 mL) at room temperature, and the mixture was allowed to stir for 30 min. Then, the solution was pumped to dryness and the residue extracted with *n*-pentane (3×5 mL). The filtrate was concentrated to 5 mL, stored at −30 °C overnight, and the resulting white precipitate washed with pentane (2×1 mL). **1** was isolated as a white powder (216.5 mg, 37% yield). $^{31}P\{^{1}H\}$ NMR ($CDCl_3$, 202.5 MHz, 298 K): $\delta=3.62$ (d, $^{4}J(P,F)=86.8$ Hz); ^{29}Si NMR ($CDCl_3$, 99.4 MHz, 298 K): $\delta=-5.2$ (d, $^{1}J(Si,F)=289$ Hz); $^{19}F\{^{1}H\}$ NMR ($CDCl_3$, 282.2 MHz, 298 K): $\delta=-144$ (d, $^{4}J(F,P)=87$ Hz); ^{1}H NMR ($CDCl_3$, 500 MHz, 298 K): $\delta=7.59$ (d, $^{3}J(H,H)=7.1$ Hz, 2H; H_{arom}), 7.56 (dd, $^{3}J(H,H)=8.0$ Hz, $^{3}J(H,H)=8.1$ Hz, 2H; H_m *Ph*), 7.46 (d, $^{3}J(H,H)=7.5$ Hz, 2H; H_{arom}), 7.42 (t, $^{3}J(H,H)=7.4$ Hz, 2H; H_{arom}), 7.38 (d, $^{3}J(H,H)=7.4$ Hz, 1H; H_o Ph), 7.31 (t, $^{3}J(H,H)=7.5$ Hz, 2H; H_p Ph), 7.25 (t, $^{3}J(H,H)=7.4$ Hz, 2H; H_{arom}), 2.09 (sept, $^{3}J(H,H)=6.9$ Hz, 2H; C*H*CH_3), 1.94 (sept, $^{3}J(H,H)=7.0$ Hz, 2H; C*H*CH_3), 1.05 (dd, $^{3}J(H,P)=7.1$ Hz, $^{3}J(H,H)=6.9$ Hz, 6H; CHC*H*$_3$), 1.04 (dd, $^{3}J(H,P)=6.4$ Hz, $^{3}J(H,H)=6.9$ Hz, 6H; CHC*H*$_3$), 0.83 (dd, $^{3}J(H,P)=5.2$ Hz, $^{3}J(H,H)=7.1$ Hz, 6H; CHC*H*$_3$), 0.75 (dd, $^{3}J(H,P)=5.5$ Hz, $^{3}J(H,H)=7.1$ Hz, 6H; CHC*H*$_3$); $^{13}C\{^{1}H\}$ NMR ($CDCl_3$, 125.8 MHz, 298 K): $\delta=145.0$ (d, $^{1}J(C,P)=19$ Hz; PC_{ipso}), 144.0 (dd, $^{2}J(C,P)=45.0$ Hz, $^{2}J(C,F)=13.5$ Hz; SiC_{ipso}), 137.5 (td, $^{2}J(C,P)=15.6$ Hz, $^{4}J(C,F)=2.8$ Hz; C_{arom}), 135.6 (s; C_m Ph), 132.1 (s; C_{arom}), 129.5 (s; C_o Ph), 129.3 (s; C_{arom}), 127.6 (s; C_{arom}), 127.4 (s; C_p Ph), 25.3 (d, $^{1}J(C,P)=14.5$ Hz; *C*HCH$_3$), 24.9 (d, $^{1}J(C,P)=14.5$ Hz; *C*HCH$_3$), 20.2 (d, $^{2}J(C,P)=12.9$ Hz; CH*C*H$_3$), 20.2 (d, $^{2}J(C,P)=18.9$ Hz; CH*C*H$_3$), 20.2 (d, $^{2}J(C,P)=10.8$ Hz; CH*C*H$_3$), 19.6 (d, $^{2}J(C,P)=16.0$ Hz; CH*C*H$_3$); HRMS (ESI+) calcd for $[M+H]^+=C_{30}H_{40}P_2FSi^+$: 511.2515, found: 511.2533.

Synthesis of 2: A solution of $SiCl_4$ (209 μL, 1.82 mmol) in toluene (5 mL) was added dropwise to a solution of *o*-lithiated diisopropylphenylphosphine (939 mg, 3.72 mmol) in toluene (10 mL) at −78 °C.The solution was allowed to warm slowly to room temperature over 4 h, after which the volatile substances were removed under vacuum, and the product was extracted with dichloromethane (15 mL). A solution of HF·collidine (284 mg, 3.64 mmol) in dichloromethane (5 mL) was added to the solution of the above product in dichloromethane (15 mL) at room temperature, the mixture was allowed to stir for 30 min. Then, the solution was pumped to dryness and the residue extracted with *n*-pentane (3×10 mL). Residual phosphonium salt was deprotonated with 1,8-diazabicyclo-[5.4.0]undec-7-ene (97 μL, 0.65 mmol) in dichloromethane (5 mL). The solution was pumped to dryness and the solid extracted with *n*-pentane (3×5 mL). Filtrates were combined and concentrated to 10 mL and stored at −30 °C overnight. **2** was isolated as a white powder (393 mg, 48% yield). Colorless crystals suitable for X-ray crystallography were obtained from pentane solution at −30 °C (see Figure S2, Supporting Information). $^{31}P\{^{1}H\}$ NMR (C_6D_6, 202.5 MHz, 298 K): $\delta=5.9$ (t, $^{4}J(P,F)=48$ Hz); ^{29}Si NMR (C_6D_6, 99.4 MHz, 298 K): $\delta=-33.1$ (t, $^{1}J(Si,F)=288$ Hz); $^{19}F\{^{1}H\}$ NMR (C_6D_6, 282.5 MHz, 298 K): $\delta=-131.1$ (t, $^{1}J(F,Si)=288$ Hz, $^{4}J(F,P)=48$ Hz); ^{1}H NMR (C_6D_6, 500 MHz; 298 K): $\delta=8.41$ (d, $^{3}J(H,H)=7.4$ Hz, 2H; H_{arom}), 7.26 (d, $^{3}J(H,H)=7.3$ Hz, 2H; H_{arom}), 7.18 (m, 2H; H_{arom}), 7.14 (m, 2H; H_{arom}), 1.83 (sept d, $^{2}J(H,P)=3.8$ Hz, $^{3}J(H,H)=7.0$ Hz, 4H; C*H*CH_3), 1.00 (dd, $^{3}J(H,P)=14.3$ Hz, $^{3}J(H,H)=7.0$ Hz, 12H; CHC*H*$_3$), 0.71 (dd, $^{3}J(H,P)=12.3$ Hz, $^{3}J(H,H)=7.0$ Hz, 12H; CHC*H*$_3$); $^{13}C\{^{1}H\}$ NMR (C_6D_6, 125.8 MHz, 301 K): $\delta=144.3$ (d, $^{2}J(C,P)=17.6$ Hz; PC_{ipso}), 142.5 (td, $^{2}J(C,P)=48.0$ Hz, $^{2}J(C,F)=16.1$ Hz, $^{4}J(C,P)=3.6$ Hz; SiC_{ipso}), 138.9 (AA'X, $N=12.7$ Hz; C_{arom}), 131.6 (s; C_{arom}), 130.5 (s; C_{arom}), 128.3 (s; C_{arom}), 25.2 (d, $^{1}J(C,P)=13.3$ Hz; *C*HCH$_3$), 20.2 (d, $^{2}J(C,P)=17.8$ Hz; CH*C*H$_3$), 20.1 (d, $^{2}J(C,P)=11.5$ Hz; CH*C*H$_3$); HRMS (ESI+) calcd for $[M+H]^+=C_{24}H_{37}P_2F_2Si^+$: 453.2133, found: 453.2108.

Synthesis of 3: A solution of $SiMeCl_3$ (137 μL, 1.17 mmol) in toluene (5 mL) was added dropwise to a solution of *o*-lithiated diisopropylphenylphosphine (621 mg, 2.46 mmol) in toluene (5 mL) at −78 °C. The solution was allowed to warm slowly to room temperature during 4 h, after which the volatile substances were removed under vacuum. Then the ligand was extracted from the salts with dichloromethane (10 mL). A solution of HF·collidine (91 mg, 1.17 mmol) in dichloromethane (5 mL) was added to a solution of the above product in dichloromethane (10 mL) at room temperature, and the mixture was allowed to stir for 30 min. Then, the solution was pumped to dryness, and the residue was extracted with *n*-pentane (3×5 mL). The filtrate was concentrated to 5 mL and stored at −30 °C overnight. **3** was isolated as a white powder (173 mg, 33% yield). $^{31}P\{^{1}H\}$ NMR ($CDCl_3$, 202.5 MHz, 298 K): $\delta=2.8$ (d, $^{4}J(P,F)=52$ Hz); ^{29}Si NMR ($CDCl_3$, 99.4 MHz, 298 K): $\delta=6.0$ (d, $^{1}J(Si,F)=279.7$ Hz); $^{19}F\{^{1}H\}$ NMR ($CDCl_3$, 282.2 MHz, 298 K): $\delta=-151$ (d, $^{4}J(F,P)=52$ Hz); ^{1}H NMR ($CDCl_3$, 500 MHz, 298 K): $\delta=7.89$ (m, 2H; H_{arom}), 7.46 (m, 2H; H_{arom}), 7.34 (m, 4H; H_{arom}), 2.00 (sept d, $^{2}J(H,P)=1.3$ Hz, $^{3}J(H,H)=6.9$ Hz, 2H; C*H*CH_3), 1.88 (sept d, $^{2}J(H,P)=3.2$ Hz, $^{3}J(H,H)=7.0$ Hz, 2H; C*H*CH_3), 1.06 (dd, $^{3}J(H,P)=14.0$ Hz, $^{3}J(H,H)=6.9$ Hz, 6H; CHC*H*$_3$), 1.03 (dt, $^{3}J(H,F)=8.1$ Hz, $^{5}J(H,P)=2.5$ Hz, 3H; SiC*H*$_3$), 0.98 (dd, $^{3}J(H,P)=13.6$ Hz, $^{3}J(H,H)=6.9$ Hz, 6H; CHC*H*$_3$), 0.70 (dd, $^{3}J(H,P)=14.8$ Hz, $^{3}J(H,H)=7.3$ Hz, 6H; CHC*H*$_3$), 0.69 (dd, $^{3}J(H,P)=14.5$ Hz, $^{3}J(H,H)=7.3$ Hz, 6H; CHC*H*$_3$); $^{13}C\{^{1}H\}$ NMR ($CDCl_3$, 125.8 MHz, 301 K): $\delta=145.9$ (dd, $^{2}J(C,F)=13.9$ Hz, $^{3}J(C,P)=44.5$ Hz; SiC_{ipso}), 143.9 (d, $^{1}J(C,P)=18.0$ Hz; PC_{ipso}), 137.1 (m, C_{arom}), 131.6 (d, $^{3}J(C,P)=2.1$ Hz; C_{arom}), 129.1 (s; C_{arom}), 127.6 (s; C_{arom}), 25.5 (d, $^{1}J(C,P)=14.0$ Hz; *C*HCH$_3$), 25.0 (d, $^{1}J(C,P)=13.0$ Hz; *C*HCH$_3$), 20.4 (d, $^{2}J(C,P)=13.1$ Hz; CH*C*H3), 20.2 (d, $^{2}J(C,P)=18.3$ Hz; CH*C*H$_3$), 20.2 (d, $^{2}J(C,P)=12.3$ Hz; CH*C*H$_3$), 19.8 (d, $^{2}J(C,P)=16.6$ Hz; CH*C*H3), 4.0 (td, $^{2}J(C,F)=16.3$ Hz, $^{4}J(C,P)=11.2$ Hz; Si*C*H$_3$); HRMS (ESI+) calcd for $[M+H]^+=C_{25}H_{40}P_2FSi$: 449.2347, found: 449.2359.

Synthesis of complex 4: A solution of **1** (79 mg, 0.15 mmol) in dichloromethane (1 mL) was added to a suspension of $AuCl(SMe_2)$ (44 mg, 0.15 mmol) in dichloromethane (1 mL) at −78 °C. After warming to room temperature, the solution was pumped to dryness and complex **4** was isolated as a white powder (98 mg, 88%). Two isomers are observed in NMR spectra: $\mathbf{4}_{trans}$ and the $\mathbf{4}_{cis}$ with the fluorine atom positioned *trans* and *cis* to gold, respectively. Colorless crystals suitable for X-ray crystallography were obtained from dichloromethane/pentane at room temperature. $\mathbf{4}_{trans}$: $^{31}P\{^{1}H\}$ NMR ($CDCl_3$, 202.5 MHz, 263 K): $\delta=57.1$ (s); ^{29}Si NMR ($CDCl_3$, 99.4 MHz, 263 K): $\delta=-21.4$ (d, $^{1}J(Si,F)=259$ Hz); $^{19}F\{^{1}H\}$ NMR ($CDCl_3$, 376.3 MHz, 213 K): $\delta=-135.8$ (s); ^{1}H NMR ($CDCl_3$, 500 MHz, 263 K): $\delta=8.26$ (d, $^{3}J(H,H)=7.5$ Hz, 2H; H_{arom}), 7.80 (d, $^{3}J(H,H)=6.9$ Hz, 2H; H_o Ph), 7.59 (d, $^{3}J(H,H)=8.2$ Hz, 2H; H_{arom}), 7.52 (m, 4H; H_{arom}), 7.35 (m, 3H; H_m and H_p Ph), 2.70 (m, 2H; C*H*CH$_3$), 2.61 (m, 2H; C*H*CH$_3$), 1.42 (m, 6H; CHC*H*$_3$), 1.13 (m, 6H; CHC*H*$_3$), 0.93 (m, 12H, CHC*H*$_3$); $^{13}C\{^{1}H\}$ NMR ($CDCl_3$, 125.8 MHz, 263 K): $\delta=144.1$ (dt, $^{2}J(C,F)=19.5$ Hz, $^{2}J(C,P)=15$ Hz; SiC_{ipso}), 137.4 (dd, $^{3}J(C,P)=9.0$ Hz, $^{3}J(C,F)=10.3$ Hz; C_{arom}), 136.9 (AA'X, $N=19.5$ Hz; PC_{ipso}), 135.5 (s; C_m Ph), 135.1 (d, $^{2}J(C,F)=23.3$ Hz; C_{ipso} *Ph*), 133.2 (s; C_o Ph), 131.1 (s; C_{arom}), 130.2 (s; C_{arom}), 129.6 (s; C_4), 128.1 (s; C_p Ph), 28.4 (AA'X, $N=$

14.0 Hz; *C*HCH$_3$), 25.4 (AA′X, N=12.9 Hz; *C*HCH$_3$), 19.4 (AA′X, N=2.4 Hz; CH*C*H$_3$),18.3 (s; CH*C*H$_3$), 16.4 (s; CH*C*H$_3$). **4**$_{cis}$: ^{31}P{^{1}H} NMR (CDCl$_3$, 202.5 MHz, 263 K): δ=59.6 (d, ^4J(P,F)=22.5 Hz); ^{29}Si NMR (CDCl$_3$,99.4 MHz, 263 K): δ=−3.9 (d, ^1J(Si,F)=318 Hz); ^{19}F{^{1}H} NMR (CDCl$_3$, 376.3 MHz, 213 K): δ=−114.9 (d, ^4J(F,P)=20 Hz); ^{1}H NMR (CDCl$_3$, 500 MHz, 263 K): δ=7.97 (d, ^3J(H,H)=7.5 Hz, 2H; H$_{arom}$), 7.80 (m, 2H; H$_{arom}$), 7.52 (m, 3H; H$_o$ Ph et H$_{arom}$), 7.46 (t, ^3J(H,H)=7.4 Hz, 2H; H$_{arom}$), 7.33 (m, 4H; H$_m$ et H$_p$ Ph), 3.00 (m, 2H, C*H*CH$_3$), 2.77 (m, 2H, C*H*CH$_3$), 1.58 (m, 6H; CHC*H*$_3$), 1.27 (m, 12H; CHC*H*$_3$), 1.00 (m, 6H; CHC*H*$_3$).^{13}C{^{1}H} NMR (CDCl$_3$, 125.8 MHz, 263 K): δ=141.3 (dd, ^2J(C,F)=9.1 Hz, ^2J(C,P)=12.9 Hz; SiC$_{ipso}$), 138.2 (t, ^2J(C,P)=7.6 Hz; C$_{arom}$), 137.7 (t, ^1J(C,P)=18.1 Hz; PC$_{ipso}$), 137.7 (d, ^2J(C,F)=14.6 Hz; SiC$_{Ph}$), 132.6 (s; C$_{arom}$), 130.0 (s; C$_o$ Ph), 129.6 (s; C$_{arom}$), 128.8 (s; C$_{arom}$), 127.8 (s; C$_p$ and C$_m$ Ph), 27.0 (AA′X, N=13.3 Hz; *C*HCH$_3$), 24.8 (AA′X, N=14.1 Hz; *C*HCH$_3$), 20.0(s; CH*C*H$_3$), 18.9 (AA′X, N=4.2 Hz; CH*C*H$_3$),18.7 (s; CH*C*H$_3$), 17.8 (s; CH*C*H$_3$); HRMS (ESI+) calcd for C$_{30}$H$_{41}$P$_2$FSiAuCl: 707.2102, found: 707.2113.

Synthesis of complex 5: A solution of **2** (150 mg, 0.33 mmol) in dichloromethane (4 mL) was added to a suspension of AuCl(SMe$_2$) (100 mg, 0.34 mmol) in dichloromethane (2 mL) at −78 °C. After warming to room temperature, the solution was pumped to dryness and complex **5** was isolated as a white powder (201 mg, 88 %). Colorless crystals suitable for X-ray crystallography were obtained from dichloromethane/diethyl ether at −30 °C. ^{31}P{^{1}H} NMR (CDCl$_3$, 202.5 MHz, 278 K): δ=63.2 (d, ^4J(P,F)=16.5 Hz); ^{29}Si NMR (CDCl$_3$,99.4 MHz, 278 K): δ=−37.3 (ps t, ^1J(Si,F)=281 Hz); ^{19}F{^{1}H} NMR (CDCl$_3$, 376.3 MHz, 213 K): δ=−108.1 (td, ^3J(P,F)=14.7 Hz, ^2J(F,F)=26 Hz; F$_{eq}$), −125.4 (d, ^2J(F,F)=26 Hz; F$_{ap}$), ^{1}H NMR (CDCl$_3$, 500 MHz, 278 K): δ=8.29 (d, ^3J(H,H)=8.0 Hz, 2H; H$_{arom}$), 7.57 (m, 6H; H$_{arom}$), 2.99 (m, 2H; C*H*CH$_3$), 2.90 (m, 2H; C*H*CH$_3$), 1.60 (m, 6H; CHC*H*$_3$), 1.26 (m, 12H; CHC*H*$_3$), 0.97 (m, 6H; CHC*H*$_3$) ^{13}C{^{1}H} NMR (CDCl$_3$, 125.8 MHz, 278 K): δ=142.1 (m, SiC$_{ipso}$), 137.9 (AA′X, N=12.2 Hz; C$_{arom}$), 136.5 (t, ^3J(C,P)=20.4 Hz, ^3J(C,F)=1.4 Hz; PC$_{ipso}$), 132.4 (s; C$_{arom}$), 130.6 (s; C$_{arom}$), 130.5 (s; C$_{arom}$), 26.6 (AA′X, N=14.1 Hz; *C*HCH$_3$), 25.3 (AA′X, N=14.7 Hz; *C*HCH$_3$), 19.9 (s; CH*C*H$_3$), 18.9 (s; CH*C*H$_3$), 18.9 (s; CH*C*H$_3$), 17.5 (s; CH*C*H$_3$); HRMS (ESI+) calcd for $[M-Cl]^+$=C$_{24}$H$_{36}$P$_2$F$_2$SiAu$^+$: 649.1682, found: 649.1695.

Synthesis of complex 6: A solution of **3** (100 mg, 0.22 mmol) in dichloromethane (4 mL) was added to a suspension of AuCl(SMe$_2$) (64 mg, 0.22 mmol) in dichloromethane (2 mL) at −78 °C. After warming to room temperature, the solution was pumped to dryness and the complex **3** was isolated as a white powder (131 mg, 87 %). Colorless crystals suitable for X-ray crystallography were obtained from THF/pentane solution at −30 °C. ^{31}P{^{1}H} NMR (CDCl$_3$, 202.5 MHz, 298 K): δ=60.1 (s); ^{29}Si NMR (CDCl$_3$,99.4 MHz, 298 K): δ=−10.2 (s, ^1J(Si,F)=267 Hz); ^{19}F{^{1}H} NMR (CDCl$_3$, 376.3 MHz, 213 K): δ=−141.5 (s); ^{1}H NMR (CDCl$_3$, 500 MHz, 298 K): δ=8.25 (d, ^3J(H,H)=7.1 Hz, 2H; H$_{arom}$), 7.51 (m, 4H; H$_{arom}$), 7.43 (t, 2H, ^3J(H,H)=7.0 Hz; H$_{arom}$), 2.89 (m, 2H; C*H*CH$_3$), 2.80 (m, 2H; C*H*CH$_3$), 1.51 (m, 6H; CHC*H*$_3$), 1.45 (d, ^3J(H,F)=11.4 Hz, 3H; SiC*H*$_3$), 1.41 (dd, ^3J(H,P)=7.8 Hz, ^3J(H,H)=6.5 Hz, 6H; CHC*H*$_3$), 1.41 (m, 6H; CHC*H*$_3$), 1.32 (m, 6H; CHC*H*$_3$), 0.88 (m, 6H; CHC*H*$_3$); ^{13}C{^{1}H} NMR (CDCl$_3$, 125.8 MHz, 298 K): δ=146.9 (dd, ^2J(C,F)=15.6 Hz, ^2J(C,P)=6.4 Hz; SiC$_{ipso}$), 136.8 (q, ^4J(C,F)=10.5 Hz, ^2J(C,P)=8.6 Hz; C$_{arom}$), 136.2 (t, ^3J(C,P)=20.5 Hz; PC$_{ipso}$), 131.6 (s; C$_{arom}$), 130.2 (s; C$_{arom}$), 129.2 (s; C$_{arom}$), 28.1 (AA′X, N=13.5 Hz; *C*HCH$_3$), 25.5 (AA′X, N=13.8 Hz; *C*HCH$_3$), 19.8 (s; CH*C*H$_3$), 19.4 (s; CH*C*H$_3$), 18.7 (s; CH*C*H$_3$), 18.4 (s; CH*C*H$_3$), 9.9 (d, J(C,F)=24.2 Hz; Si*C*H$_3$); HRMS (ESI+) calcd for $[M-Cl]^+$=C$_{25}$H$_{39}$P$_2$FSiAu$^+$: 645.1924, found: 645.1946.

Synthesis of 7: A solution of Me$_2$SiCl$_2$ (115 μL, 0.94 mmol) in toluene (5 mL) was added dropwise to a solution of *o*-lithiated diisopropylphenylphosphine (475 mg, 1.88 mmol) in toluene (5 mL) at −78 °C. The solution was allowed to warm slowly to room temperature overnight, after which the volatile substances were removed under vacuum, and ligand **7** was extracted from the salts with dichloromethane (10 mL). Then, the solution was pumped to dryness, and the residue crystallized from *n*-pentane (5 mL). **7** was isolated as a white powder (177.7 mg, 42 % yield). ^{31}P{^{1}H} NMR (C$_6$D$_6$, 202.5 MHz, 301 K): δ=1.3 (s); ^{29}Si NMR (C$_6$D$_6$, 99.4 MHz, 301 K): δ=−7.0 (s); ^{1}H NMR (C$_6$D$_6$, 500 MHz, 301 K): δ=7.96 (m, 2H; H$_{arom}$), 7.49 (m, 2H; H$_{arom}$), 7.28 (m, 4H; H$_{arom}$), 1.93 (sept d, ^2J(H,P)=4.3 Hz, ^3J(H,H)=7.0 Hz, 4H; C*H*CH$_3$), 1.20 (t, ^5J(H,P)=1.6 Hz, 6H; Si(C*H*$_3$)$_2$), 1.17 (dd, ^3J(H,P)=13.2 Hz, ^3J(H,H)=6.9 Hz, 12H; CHC*H*$_3$), 0.92 (dd, ^3J(H,P)=12.9 Hz, ^3J(H,H)=7.1 Hz, 12H; CHC*H*$_3$); ^{13}C{^{1}H} NMR (C$_6$D$_6$, 125.8 MHz, 301 K): δ=148.9 (dd, ^1J(C,P)=43.9 Hz, ^4J(C,P)=1.7 Hz; PC$_{ipso}$), 144.9 (d, ^2J(C,P)=17.8 Hz; PC$_{ipso}$), 137.1 (dd, ^2J(C,P)=15.1 Hz, ^6J(C,P)=3.4 Hz; C$_{arom}$), 132.0 (d, ^3J(C,P)=2.2 Hz; C$_{arom}$), 128.3 (s; C$_{arom}$), 128.0 (signal overlapped by the C$_6$D$_6$ signals), 25.9 (d, ^1J(C,P)=14.8 Hz; *C*HCH$_3$), 21.0 (d, ^1J(C,P)=14.1 Hz; *C*HCH$_3$), 20.2 (d, ^2J(C,P)=17.7 Hz; CH*C*H$_3$), 5.3 (t, ^2J(C,P)=12.5 Hz; Si(*C*H$_3$)$_2$); HRMS (ESI+) calcd for $[M+H]^+$=C$_{26}$H$_{43}$P$_2$Si$^+$: 445.2609, found: 445.2613.

Synthesis of complex 8: A solution of **7** (120 mg, 0.27 mmol) in dichloromethane (1 mL) was added to a suspension of AuCl(SMe$_2$) (79.2 mg, 0.27 mmol) in dichloromethane (1 mL) at −78 °C. After warming to room temperature, the solution was pumped to dryness and complex **8** was isolated as a white powder (157.8 mg, 86 %). Colorless crystals suitable for X-ray crystallography were obtained from dichloromethane/pentane at room temperature. ^{31}P{^{1}H} NMR (C$_6$D$_6$, 121.4 MHz, 298 K): δ=53.98 (s); ^{29}Si NMR (CDCl$_3$, 59.6 MHz, 298 K): δ=−12.4 (s); ^{1}H NMR (CDCl$_3$, 300 MHz, 298 K): δ=7.79 (m, 2H; H$_{arom}$), 7.05 (m, 6H; H$_{arom}$), 2.41 (sept d, ^2J(H,P)=3.5 Hz, ^3J(H,H)=6,9 Hz, 4H; C*H*CH$_3$), 1.30 (dd, ^3J(H,P)=15.2 Hz, ^3J(H,H)=8.2 Hz, 12H; CHC*H*$_3$), 1.02 (dd, ^3J(H,P)=15.6 Hz, ^3J(H,H)=8.2 Hz, 12H; CHC*H*$_3$), 0.98 (s; 6H; Si(C*H*$_3$)$_2$); ^{13}C{^{1}H} NMR (CDCl$_3$, 75.4 MHz, 298 K): δ=147.7 (AA′X, N=15.1 Hz; C$_{ipso}$), 139.1 (AA′X, N=18.0 Hz; C$_{ipso}$), 137.3 (AA′X, N=7.9 Hz; C$_{arom}$), 131.7 (s; C$_{arom}$), 129.0 (s; C$_{arom}$), 128.2(s; C$_{arom}$), 27.7 (AA′X, N=12.5 Hz; *C*HCH$_3$), 19.5 (AA′X, N=2.6 Hz; *C*HCH$_3$), 18.8 (AA′X, N=2.8 Hz; CH*C*H$_3$), 8.6 (t, ^4J(C,P)=2.3 Hz; Si(*C*H$_3$)$_2$); HRMS (ESI+) calcd for $[M-Cl]^+$=C$_{26}$H$_{42}$P$_2$SiAu$^+$: 641.2197, found: 641.2222.

EXSY experiments: 2D ^{31}P{^{1}H} EXSY spectra were recorded in CDCl$_3$ at 277 K for complex **4**, and 2D ^{19}F EXSY spectra in CDCl$_3$ at 223, 243, 273, 283 and 303 K for complex **5**, with a phase sensitive pulse sequence from the Bruker pulse library NOESYTP. The EXSY measurements were repeated with a series of mixing times τ_m=20 μs and 0.3 s at 277 K for **4**, and τ_m=10 μs, 0.3 s, and 0.5 s at 223, 243, 273, 283 and 303 K for complex **5**. The diagonal and cross-peak volumes were integrated with Bruker 2D WINNMR software. Site-to-site rate constants were determined by using the EXSY CALC software from Mestrelab Research. Activation barriers were then calculated by using the Eyring equation.

Crystal structure determinations: The X-ray diffraction structures of **1** and **4** were reported in a preliminary communication.[11]

Crystallographic data were collected on Bruker-Kappa APEX-II diffractometer (for **5** and **6**) and Bruker-AXS APEX-II diffractometer (for **2** and **8**) with Mo$_{K\alpha}$ radiation (λ=0.71073 Å) at 180(2) K for **5**, 100(2) K for **6**, and 193(2) K for **2** and **8**. In all cases, a suitable crystal was mounted on a glass fiber or nylon loop and shock-cooled on the goniometer head. Semi-empirical absorption corrections were employed.[26] The structures were solved by direct methods (SHELXS-97),[27] and refined using the least-squares method on F^2.[28]

Crystal data for **2**: C$_{24}$H$_{36}$F$_2$P$_2$Si, M=452.56, monoclinic, space group *C*2, a=11.8945(7), b=12.2407(5), c=9.2210(5) Å, α=90, β=109.374(3), γ=90, V=1266.53(11) Å^3, Z=2, ρ_{calcd}=1.187 g cm^{-3}, F(000)=484, T=193(2) K, crystal size 0.40×0.20×0.02 mm^3, 3772 reflections collected (2329 independent, R_{int}=0.0389), $2\theta \le 26.37°$, 136 parameters, $R1$ [$I>2\sigma(I)$]=0.0461, $wR2$ (all data)=0.0595, largest diff. peak and hole: 0.225 and −0.189 e Å^{-3}.

Crystal data for **5**: C$_{24}$H$_{36}$AuClF$_2$P$_2$Si, M=684.98, monoclinic, space group $P2_1/c$, a=11.5749(6), b=15.0010(8), c=31.6610(17) Å, α=90, β=98.240(2), γ=90, V=5440.7(5) Å^3, Z=8, ρ_{calcd}=1.672 g cm^{-3}, F(000)=2704, T=180(2) K, crystal size 0.283×0.113×0.03 mm^3, 77767 reflections collected (13085 independent, R_{int}=0.0864), $2\theta \le 27.88°$, 577 parameters, $R1$ [$I>2\sigma(I)$]=0.0660, $wR2$ (all data)=0.1418, largest diff. peak and hole: 2.927 and −3.708 e Å^{-3}.

Crystal data for **6**: C$_{25}$H$_{39}$AuClFP$_2$Si, M=681.01, monoclinic, space group $P2_1/c$, a=11.5556(3), b=14.9979(4), c=31.9588(8) Å, α=90, β=97.3890(10), γ=90°, V=5492.8(2) Å^3, Z=8, ρ_{calcd}=1.647 g cm^{-3}, F(000)=

2704, $T=100(2)$ K, crystal size $0.23\times0.08\times0.03$ mm^3, 13085 reflections collected (12960 independent, $R_{int}=0.0864$), $2\theta\leq27.88°$, 577 parameters, $R1$ $[I>2\sigma(I)]=0.0999$, $wR2$ (all data) $=0.1418$, largest diff. peak and hole: 2.927 and -3.708 e Å^{-3}.

Crystal data for **8**: $C_{26}H_{42}AuClP_2Si$, $M=705.1$, orthorhombic, space group $P21\ 21\ 21$, $a=8.9619(1)$, $b=12.0314(2)$, $c=29.6707(4)$ Å, $\alpha=90$, $\beta=90$, $\gamma=90°$, $V=3199.22(8)$ Å^3, $Z=4$, $\rho_{calcd}=1.582$ g cm^{-3} $F(000)=1520$, $T=180(2)$ K, crystal size $0.22\times0.08\times0.06$ mm^3, 49291 reflections collected (9725 independent, $R_{int}=0.0458$), $2\theta\leq30.49°$, 318 parameters, $R1$ $[I>2\sigma(I)]=0.0276$, $wR2$ (all data) $=0.0525$, largest diff. peak and hole: 1.264 and -1.050 e Å^{-3}.

CCDC-776015 (**2**), 776016 (**5**), 776017 (**6**), and 776018 (**8**) contain the supplementary crystallographic data for this paper. These data can be obtained free of charge from The Cambridge Crystallographic Data Centre via www.ccdc.cam.ac.uk/data_request/cif.

Computational details: Calculations were carried out on the actual complexes **4**, **5**, **6**, and **8**. Au, P, and Cl were treated with a Stuttgart–Dresden pseudopotential in combination with their adapted basis set.[29–31] In all cases, the basis set was augmented by a set of polarization function (f for Au, d for P and Cl).[32] C, H, Si and F atoms were described with a 6-31G-(d,p) double-ζ basis set.[33] Calculations were carried out at the DFT level of theory with the hybrid functional B3PW91.[34–35] Geometry optimizations were carried out without any symmetry restrictions, the nature of the extrema was verified with analytical frequency calculations. All computations were performed with the Gaussian 03[36] suite of programs. The electronic structure of the complexes was studied by Natural Bond Orbital (NBO) analysis (NBO 3.1 program),[37–38] second-order perturbation theory being particularly adapted to the description of metal→Lewis acid interactions. The electron density of the optimized structures of complexes **4**, **5**, **6** and **8** was subjected to an Atoms In Molecules analysis[39] with AIM2000.[40]

Acknowledgements

Financial support from the Centre National de la Recherche Scientifique, the Pôle de Recherche et d'Enseignement Supérieur of the Université de Toulouse (fellowship to P.G.) and the COST action CM0802 PhoSciNet is gratefully acknowledged. We thank the Unidade de RaiosX of the Universidade de Santiago de Compostela for the X-ray diffraction analysis of **6**, Pierre Lavedan for the 2D ^{19}F EXSY NMR experiments on complex **5**, and François Gabbaï for helpful discussions. L.M. thanks the Institut Universitaire de France.

[1] a) R. B. King, *Adv. Chem. Ser.* **1967**, *62*, 203–220; b) M. L. H. Green, *J. Organomet. Chem.* **1995**, *500*, 127–148.

[2] a) H. Braunschweig, C. Kollann, D. Rais, *Angew. Chem.* **2006**, *118*, 5380–5400; *Angew. Chem. Int. Ed.* **2006**, *45*, 5254–5274; b) F. G. Fontaine, J. Boudreau, M. H. Thibault, *Eur. J. Inorg. Chem.* **2008**, 5439–5454; c) I. Kuzu, I. Krummenacher, J. Meyer, F. Armbruster, F. Breher, *Dalton Trans.* **2008**, 5836–5865; d) H. Braunschweig, R. D. Dewhurst, A. Schneider, *Chem. Rev.* **2010**, *110*, 3924–3957.

[3] For a dative Pt→Be, see: a) H. Braunschweig, K. Gruss, K. Radacki, *Angew. Chem.* **2009**, *121*, 4303–4305; *Angew. Chem. Int. Ed.* **2009**, *48*, 4239–4241.

[4] a) S. Bontemps, H. Gornitzka, G. Bouhadir, K. Miqueu, D. Bourissou, *Angew. Chem.* **2006**, *118*, 1641–1644; *Angew. Chem. Int. Ed.* **2006**, *45*, 1611–1614; b) S. Bontemps, G. Bouhadir, K. Miqueu, D. Bourissou, *J. Am. Chem. Soc.* **2006**, *128*, 12056–12057; c) S. Bontemps, G. Bouhadir, P. W. Dyer, K. Miqueu, D. Bourissou, *Inorg. Chem.* **2007**, *46*, 5149–5151; d) M. Sircoglou, S. Bontemps, M. Mercy, N. Saffon, M. Takahashi, G. Bouhadir, L. Maron, D. Bourissou, *Angew. Chem.* **2007**, *119*, 8737–8740; *Angew. Chem. Int. Ed.* **2007**, *46*, 8583–8586; e) S. Bontemps, M. Sircoglou, G. Bouhadir, H. Puschmann, J. A. K. Howard, P. W. Dyer, K. Miqueu, D. Bourissou, *Chem. Eur. J.* **2008**, *14*, 731–740; f) S. Bontemps, G. Bouhadir, W. Gu, M. Mercy, C.-H. Chen, B. M. Foxman, L. Maron, O. V. Ozerov, D. Bourissou, *Angew. Chem.* **2008**, *120*, 1503–1506; *Angew. Chem. Int. Ed.* **2008**, *47*, 1481–1484; g) M. Sircoglou, S. Bontemps, G. Bouhadir, N. Saffon, K. Miqueu, W. Gu, M. Mercy, C.-H. Chen, B. M. Foxman, L. Maron, O. V. Ozerov, D. Bourissou, *J. Am. Chem. Soc.* **2008**, *130*, 16729–16738; h) M. Sircoglou, M. Mercy, N. Saffon, Y. Coppel, G. Bouhadir, L. Maron, D. Bourissou, *Angew. Chem.* **2009**, *121*, 3506–3509; *Angew. Chem. Int. Ed.* **2009**, *48*, 3454–3457.

[5] In addition to η^1-coordination of boranes as acceptor ligands, multicenter η^3-BCC and η^2-BC interactions involving a π system at boron have been also evidenced: a) S. R. Oakley, K. D. Parker, D. J. H. Emslie, I. Vargas-Baca, C. M. Robertson, L. E. Harrington, J. F. Britten, *Organometallics* **2006**, *25*, 5835–5838; b) D. J. H. Emslie, L. E. Harrington, H. A. Jenkins, C. M. Robertson, J. F. Britten, *Organometallics* **2008**, *27*, 5317–5325; c) K. B. Kolpin, D. J. H. Emslie, *Angew. Chem.* **2010**, *122*, 2776–2779; *Angew. Chem. Int. Ed.* **2010**, *49*, 2716–2719; d) M. Sircoglou, S. Bontemps, M. Mercy, K. Miqueu, S. Ladeira, N. Saffon, L. Maron, G. Bouhadir, D. Bourissou, *Inorg. Chem.* **2010**, *49*, 3983–3990; e) X. Zhao, E. Otten, D. Song, D. W. Stephan, *Chem. Eur. J.* **2010**, *16*, 2040–2044.

[6] a) D. Kost, I. Kalikhman in *The Chemistry of Organic Silicon Compounds, Vol. 2, Part 2* (Eds.: Z. Rappoport, Y. Apeloig),Wiley, New York, **1998**, pp. 1339–1445; b) *Chemistry of Hypervalent Compounds*, (Ed.: K.-y. Akiba), Wiley-VCH, Weinheim, **1999**; c) Y. I. Baukov, S. N. Tandura in *The Chemistry of Organic Germanium, Tin and Lead Compounds, Vol. 2* (Ed.: Z. Rappoport), Wiley, New York, **2002**, pp. 961–1239; d) R. R. Holmes, *Chem. Rev.* **1996**, *96*, 927–950; e) C. Chuit, R. J. P. Corriu, C. Reye, J. Colin Young, *Chem. Rev.* **1993**, *93*, 1371–1448.

[7] a) J. Grobe, N. Krummen, R. Wehmschulte, B. Krebs, M. Laege, *Z. Anorg. Allg. Chem.* **1994**, *620*, 1645–1658; b) J. Grobe, R. Wehmschulte, B. Krebs, M. Laege, *Z. Anorg. Allg. Chem.* **1995**, *621*, 583–596; c) J. Grobe, K. Luetke-Brochtrup, B. Krebs, M. Laege, H. H. Niemeyer, E. U. Wuerthwein, *Z. Naturforsch. B* **2007**, *62*, 55–65.

[8] a) J. Silver, *J. Chem. Soc. Dalton Trans.* **1990**, 3513–3516; b) R. Rulkens, A. J. Lough, I. Manners, *Angew. Chem.* **1996**, *108*, 1929–1931; *Angew. Chem. Int. Ed. Engl.* **1996**, *35*, 1805–1807; c) D. L. Zechel, K. C. Hultzsch, R. Rulkens, D. Balaishis, Y. Ni, J. K. Pudelski, A. J. Lough, I. Manners, *Organometallics* **1996**, *15*, 1972–1978.

[9] a) L. Guo, J. D. Bradshaw, C. A. Tessier, W. J. Youngs, *Organometallics* **1995**, *14*, 586–588; b) L. Guo, J. D. Bradshaw, D. B. McConville, C. A. Tessier, W. J. Youngs, *Organometallics* **1997**, *16*, 1685–1692.

[10] a) J. Wagler, A. F. Hill, T. Heine, *Eur. J. Inorg. Chem.* **2008**, 4225–4229; b) J. Wagler, E. Brendler, *Angew. Chem.* **2010**, *122*, 634–637; *Angew. Chem. Int. Ed.* **2010**, *49*, 624–627.

[11] P. Gualco, T. P. Lin, M. Sircoglou, M. Mercy, S. Ladeira, G. Bouhadir, L. M. Perez, A. Amgoune, L. Maron, F. P. Gabbai, D. Bourissou, *Angew. Chem.* **2009**, *121*, 10076–10079; *Angew. Chem. Int. Ed.* **2009**, *48*, 9892–9895.

[12] The free energy of activation at coalescence temperature is typically estimated through the following formula: $\Delta G^{\neq}=RT_c\ln[RT_c\sqrt{2}/(\pi N_A h|\nu_A-\nu_B|)]$ with R (gas constant), T_c (coalescence temperature), N_A (Avogadro's number), h (Planck's constant) and $|\nu_A-\nu_B|$ (chemical shift difference): L. M. Jackman, *Dyn. Mass Spectrom.* **1975**, 203–252.

[13] a) K. G. Orrell, *Annu. Rep. NMR Spectrosc.* **1999**, *37*, 1–74; b) C. L. Perrin, T. J. Dwyer, *Chem. Rev.* **1990**, *90*, 935–967.

[14] M. Gromova, O. Jarjayes, S. Hamman, R. Nardin, C. Béguin, R. Willem, *Eur. J. Inorg. Chem.* **2000**, 545–550.

[15] C. L. Perrin, R. K. Gipe, *J. Am. Chem. Soc.* **1984**, *106*, 4036–4038.

[16] B. Cordero, V. Gómez, A. E. Pletro-Prats, M. Revés, J. Echeverría, E. Cremades, F. Barragán, S. Alvarez, *Dalton Trans.* **2008**, 2832–2838.

[17] S. S. Batsanov, *Inorg. Mater.* **2001**, *37*, 871–885.

[18] a) N. Kano, F. Komatsu, M. Yamamura, T. Kawashima, *J. Am. Chem. Soc.* **2006**, *128*, 7097–7109; b) F. Carré, R. J. P. Corriu, A. Kpoton, M. Poirier, G. Royo, J. C. Young, C. Belin, *J. Organomet. Chem.* **1994**, *470*, 43–57; c) K. Gerhard, H. Karl, F. Hartmut, *Chem. Ber.* **1983**, *116*, 3125–3132.

[19] See the Supporting Information.

[20] a) G. I. Nikonov, *Adv. Organomet. Chem.* **2005**, *53*, 217–309; b) M. Brookhart, M. L. H. Green, G. Parkin, *Proc. Natl. Acad. Sci. USA* **2007**, *104*, 6908–6914; c) D. V. Gutsulyak, S. F. Vyboishchikov, G. I. Nikonov, *J. Am. Chem. Soc.* **2010**, *132*, 5950–5951; d) S. Lachaize, S. Sabo-Etienne, *Eur. J. Inorg. Chem.* **2006**, 2115–2127; e) Z. Lin, *Chem. Soc. Rev.* **2002**, *31*, 239–245.
[21] a) W. Chen, S. Shimada, M. Tanaka, *Science* **2002**, *295*, 308–310; b) R. H. Crabtree, *Science* **2002**, *295*, 288–289; c) E. C. Sherer, C. R. Kinsinger, B. L. Kormos, J. D. Thompson, C. J. Cramer, *Angew. Chem.* **2002**, *114*, 2033–2036; *Angew. Chem. Int. Ed.* **2002**, *41*, 1953–1956; d) G. Aullón, A. Lledos, S. Alvarez, *Angew. Chem.* **2002**, *114*, 2036–2039; *Angew. Chem. Int. Ed.* **2002**, *41*, 1956–1959; e) G. I. Nikonov, *Angew. Chem.* **2003**, *115*, 1375–1377; *Angew. Chem. Int. Ed.* **2003**, *42*, 1335–1337.
[22] J. Y. Corey, J. Braddock-Wilking, *Chem. Rev.* **1999**, *99*, 175–292.
[23] a) G. Balázs, L. J. Gregoriades, M. Scheer, *Organometallics* **2007**, *26*, 3058–3075; b) R. Waterman, P. G. Hayes, T. D. Tilley, *Acc. Chem. Res.* **2007**, *40*, 712–719; c) A. C. Filippou, C. Oleg, K. W. Stumpf, G. Schnakenburg, *Angew. Chem.* **2010**, *122*, 3368–3372; *Angew. Chem. Int. Ed.* **2010**, *49*, 3296–3300.
[24] a) M. C. MacInnis, D. F. MacLean, R. J. Lundgren, R. McDonald, L. Turculet, *Organometallics* **2007**, *26*, 6522–66525; b) S. J. Mitton, R. MacDonald, L. Turculet, *Organometallics* **2009**, *28*, 5122–5136; c) S. J. Mitton, R. McDonald, L. Turculet, *Angew. Chem.* **2009**, *121*, 8720–8723; *Angew. Chem. Int. Ed.* **2009**, *48*, 8568–8571; d) E. Morgan, D. F. MacLean, R. McDonald, L. Turculet, *J. Am. Chem. Soc.* **2009**, *131*, 14234–14236; e) J. Takaya, N. Iwasawa, *J. Am. Chem. Soc.* **2008**, *130*, 15254–15255; f) J. Takaya, N. Iwasawa, *Organometallics* **2009**, *28*, 6636–6638.
[25] a) *Nuclear Magnetic Resonance Spectroscopy*, (Ed.: F. A. Bovey), Academic Press, New York, **1969**; b) R. J. Abraham, H. Berstein, *Can. J. Chem.* **1961**, *39*, 216–230.
[26] SADABS, Program for data correction, Bruker-AXS.
[27] G. M. Sheldrick, *Acta Crystallogr. Sect. A* **1990**, *46*, 467–473.
[28] SHELXL-97, Program for Crystal Structure Refinement, G. M. Sheldrick, University of Göttingen (Germany), **1997**.
[29] B. Metz, H. Stoll, M. Dolg, *J. Chem. Phys.* **2000**, *113*, 2563–2569.
[30] D. Andrae, U. Haeussermann, M. Dolg, H. Stoll, H. Preuss, *Theor. Chim. Acta* **1990**, *77*, 123–141.
[31] A. Bergner, M. Dolg, W. Kuechle, H. Stoll, H. Preuss, *Mol. Phys.* **1993**, *80*, 1431–1441.
[32] A. W. Ehlers, M. Böhme, S. Dapprich, A. Gobbi, A. Höllwarth, V. Jonas, K. F. Köhler, R. Stegmann, A. Veldkamp, G. Frenking, *Chem. Phys. Lett.* **1993**, *208*, 111–114.
[33] P. C. Hariharan, J. A. Pople, *Theor. Chim. Acta* **1973**, *28*, 213–222.
[34] A. D. Becke, *J. Chem. Phys.* **1993**, *98*, 5648–5652.
[35] K. Burke, J. P. Perdew, W. Yang, *Electronic Density Functional Theory: Recent Progress and New Directions* (Eds.: J. F. Dobson, G. Vignale, M. P. Das), Springer, Heidelberg, **1998**.
[36] Gaussian 03, Revision C.02, M. J. Frisch, G. W. Trucks, H. B. Schlegel, G. E. Scuseria, M. A. Robb, J. R. Cheeseman, V. G. Zakrzewski, J. A. Montgomery, Jr., R. E. Stratman, J. C. Burant, S. Dapprich, J. M. Millam, A. D. Daniels, K. N. Kudin, M. C. Strain, O. Farkas, J. Tomasi, V. Barone, M. Cossi, R. Cammi, B. Mennucci, C. Pomelli, C. Adamo, S. Clifford, J. Ochterski, G. A. Petersson, P. Y. Ayala, Q. Cui, K. Morokuma, D. K. Malick, A. D. Rabuck, K. Raghavachari, J. B. Foresman, J. Cioslowswi, J. V. Ortiz, A. G. Baboul, B. B. Stefanov, G. Liu, A. Liashenko, P. Piskorz, I. Komaromi, R. Gomperts, R. Martin, D. J. Fox, T. Keith, M. A. Al-Laham, C. Y. Peng, A. Nanayakkara, C. Gonzalez, M. Challacombe, P. M. W. Gill, B. Jonhson, W. Chen, M. W. Wong, J. L. Andres, M. Head-Gordon, E. S. Replogle, J. A. Pople, Pittsburgh PA, **2006**.
[37] NBO version 3.1, E. D. Glendening, A. E. Reed, J. E. Carpenter, F. Weinhold.
[38] A. E. Reed, L. A. Curtiss, F. Weinhold, *Chem. Rev.* **1988**, *88*, 899–926.
[39] R. F. W. Bader, *Atoms in Molecules: A Quantum Theory*, Oxford University Press, Oxford, **1994**.
[40] F. B. Konig, J. Schonbohm, D. Bayles, *J. Comput. Chem.* **2001**, *22*, 545–559.

Received: May 12, 2010
Published online: July 30, 2010

